frontiers | Frontiers in Earth Science

TYPE Original Research
PUBLISHED 10 April 2025
DOI 10.3389/feart.2025.1569084

Check for updates

OPEN ACCESS

EDITED BY
Hongjian Zhu,
Yanshan University, China

REVIEWED BY
Zhongying Han,
China University of Petroleum, China
Anmin Wang,
China University of Mining and Technology, Beijing, China
Moise Luemba Luemba,
University of Kinshasa, Democratic Republic of Congo

*CORRESPONDENCE
Youjun Tang,
tyj@yangtzeu.edu.cn
Xingqiang Feng,
286484521@qq.com

RECEIVED 31 January 2025
ACCEPTED 07 March 2025
PUBLISHED 10 April 2025

CITATION
Huo S, Tang Y, Qian Z, Feng X and Mei Y (2025) Study on the evaluation of fault stability and its influencing factors in rongchang area. *Front. Earth Sci.* 13:1569084.
doi: 10.3389/feart.2025.1569084

Study on the evaluation of fault stability and its influencing factors in rongchang area

Shaowei Huo[1,2], Youjun Tang[1]*, Zhuliang Qian[3], Xingqiang Feng[2,4]* and Yahao Mei[1,2]

[1]College of Resource and Environment, Yangtze University, Wuhan, China, [2]China Institute of Geomechanics, Chinese Academy of Geological Sciences, Beijing, China, [3]Geophysical Prospecting Research Institute of Jiangsu Oilfield Company, Sinopec, Nanjing, China, [4]Key Laboratory of Petroleum Geomechanics, China Geological Survey, Beijing, China

The Rongchang area, boasting abundant shale gas resources, has emerged as a pivotal region for reserve augmentation and production increase. Influenced by the Huayingshan Fault Zone, a multitude of faults have developed within this area. During the shale gas development process, the injection of high - pressure fluids and hydraulic fracturing operations are likely to trigger alterations in the stress field adjacent to the faults, thereby exerting an impact on the fault stability. Through the comprehensive utilization of geological and geophysical data, this research delves deeply into the contemporary in - situ stress environment of the Wufeng - Longmaxi Formation in the study area. In combination with the Coulomb criterion, it assesses the stability of the faults in the study area and probes into the factors influencing fault stability. The findings reveal that the contemporary in - situ stress relationship in the study area is characterized by SHmax > Sv > Shmin, placing it in a strike - slip stress environment. The evaluation of fault stability demonstrates that the faults in the western and southern parts of the study area exhibit poor stability, while those in the northeastern part possess relatively better stability. Moreover, it has been discovered that there exist disparities in stability along the same fault. There is a necessity to establish a fault model to further explore the stability factors. The results indicate that in the study area, faults with a dip angle of occurrence less than 10°, as well as those with an azimuth angle less than 30° and a dip angle greater than 60°, enjoy good stability. Conversely, for faults with an azimuth angle exceeding 50°, their stability diminishes as the dip angle increases. When the azimuth angle reaches 70° and the dip angle is greater than 70°, the stability is rather poor. This clearly indicates that the occurrence of faults stands as a crucial factor influencing fault stability. As the pore pressure rises, the range of azimuth angles and dip angles of potentially unstable faults gradually expands, signifying that pore pressure is also an essential factor affecting fault stability. This research furnishes a theoretical foundation for circumventing potential risks and attaining efficient development during the shale gas development process.

KEYWORDS

Rongchang area, fault stability, in-situ stress simulation, fault occurrence, pore pressure

1 Introduction

The Wufeng Formation-Longmaxi Formation shale in the Rongchang area has a large development thickness, with high-quality geological conditions for shale gas reservoirs and huge resource potential, making it a key area for future shale gas exploration and development (Lei, et al., 2014). Since multiple faults in the southern section of the Huayingshan Fault Zone run through the study area, the instability of faults may trigger earthquakes, leading to damage to the integrity of the shale gas reservoir, reducing the permeability and productivity of the reservoir, and further causing the deformation of the wellbore and increasing the development cost. Therefore, the stability of the faults in the study area has an important impact on the efficient development of shale gas.

The target reservoir, the Wufeng Formation-Longmaxi Formation shale geological layers in the Rongchang area, are mostly within the depth range of 2000–3,500 m. The TOC values in the shale geological layers are generally between 1.5% and 5%; the reservoir has a relatively high porosity, usually at 2%, presenting high-quality reservoir conditions. Different degrees of research have been carried out on the factors of fault stability. Zhang's suggested that seismic activity alters the regional stress field to some extent, leading to fault sliding (Zhang, et al., 2024). Yi's conducted a preliminary analysis of the seismic source structure and tectonic deformation characteristics in the Rongxian-Weiyuan-Zizhong region, identifying the stress state and deformation patterns of the seismogenic structures and highlighting the distinct regional characteristics of these patterns (Yi, et al., 2020; Yi, et al., 2019). Li's suggested that the earthquakes in the southeastern Sichuan region are the result of local stress field disturbances, which trigger the activity of detachment layers and the thrust motion of overlying blind faults. They also noted a certain temporal and spatial correlation with local industrial activities, hypothesizing that these seismic events may be closely related to resource extraction activities (Li, et al., 2022). Zhang's argued that hydraulic fracturing operations for shale gas and associated wastewater reinjection significantly increase seismic activity in the exploration area (Zhang, et al., 2021).

The above research shows that previous studies mainly used natural seismic events, focal mechanisms, and the spatiotemporal relationship of earthquakes to study the stress changes before and after earthquakes that lead to fault slippage, and there has been no research on the evaluation of fault stability by fault occurrence and its influence. Therefore, this study selects the southern section of the Huayingshan Fault in the Rongchang area as the research object, uses geological, geophysical, geomechanical and other data for three-dimensional *in-situ* stress simulation, and combines the Coulomb fault slip theory to carry out a stability evaluation of the faults in the study area. Based on the evaluation results, it simulates the influence of different fault occurrences and pore pressures on stability, which is of great significance for avoiding potential risks during the development of shale gas in the Rongchang area and for the exploration and development of shale gas.

2 Geological background

The Sichuan Basin is bounded by the Huayingshan Fault Zone and the Longquanshan Fault Zone. To the west of the Longquanshan Fault Zone is the Western Sichuan Depression tectonic area; to the east of the Huayingshan Fault Zone is the Eastern Sichuan Fold tectonic area; the area between the two is the Central Sichuan Gentle Uplift area, which is characterized by broad and gentle anticline and syncline structures (Liu, et al., 2024; Jiang, et al., 2023; Zhang, et al., 2019). The study area is located in the transition zone from the Central Sichuan Gentle Uplift area to the Eastern Sichuan Fold tectonic area. It is adjacent to Dazu County in the north, Weiyuan in the west, and Luzhou in the south. The basement fault of Huayingshan runs through the study area, and multiple faults have developed within the area. The southern end of the Huayingshan Fault shows a convergence in the northeast direction and a divergence in the southwest direction, presenting a broom-shaped distribution pattern, and the faults in the upper strata develop in a hereditary manner. During the period of neotectonic movement, the Yibin-Rongchang Fault in the middle and southern sections of the Huayingshan Fault strongly reactivated with right-lateral strike-slip movement, becoming an important seismogenic fault (Ju et al., 2027; Jiang, et al., 2024; Jiang, 2021) (Figure 1).

3 Research methods

In the field of geomechanics, *in-situ* stress calculation and Coulomb's fault slip theory are important methods for analyzing fault stability. Firstly, using Huang Rongzun's model [Equations 1, 2], based on the results of *in-situ* stress tests, it is calculated that εH is 0.0021 and εh is 0.0014. The finite element numerical simulation method is adopted to calculate the *in-situ* stress of the study area (Jiang, et al., 2023; Zheng, et al., 2017; Liu, et al., 2009; Zhou, et al., 2007). Furthermore, by using the failure function CFF (Coulomb failure function) defined by Coulomb [Equations 3–5], and combining with the friction slip tests on the samples of the Longmen Shan Fault Zone conducted by He Changrong and others, it is concluded that the friction coefficient μ of the natural fault gouge is between 0.3 and 0.4 (Zhu, et al., 2024; He and SPIERS, 2011; Zhou, et al., 2007; Zoback, et al., 2003). In this study, the minimum friction coefficient $\mu = 0.3$ is selected for analysis to explore the stability differences among faults with different occurrences, so as to analyze the stability of the faults.

$$SHmax = \left(\frac{\nu}{1-\nu} + \varepsilon_H\right)\left(S_v - \alpha P_p\right) + \alpha P_p \tag{1}$$

$$Shmin = \left(\frac{\nu}{1-\nu} + \varepsilon_h\right)\left(S_v - \alpha P_p\right) + \alpha P_p \tag{2}$$

In the formula, *SHmax* and *Shmin* are the maximum and minimum horizontal principal stresses respectively; *Pp* is the formation pore pressure, in MPa; *Sv* is the vertical stress, in MPa; ν is the Poisson's ratio, dimensionless; α is the Biot coefficient, dimensionless; εH and εh are the tectonic stress coefficients of the maximum and minimum horizontal principal stresses respectively, dimensionless.

$$\tau/\sigma_n = \mu \tag{3}$$

$$\sigma_n = S_n - P_p \tag{4}$$

$$CFF = \tau - \mu\left(S_n - P_p\right) \tag{5}$$

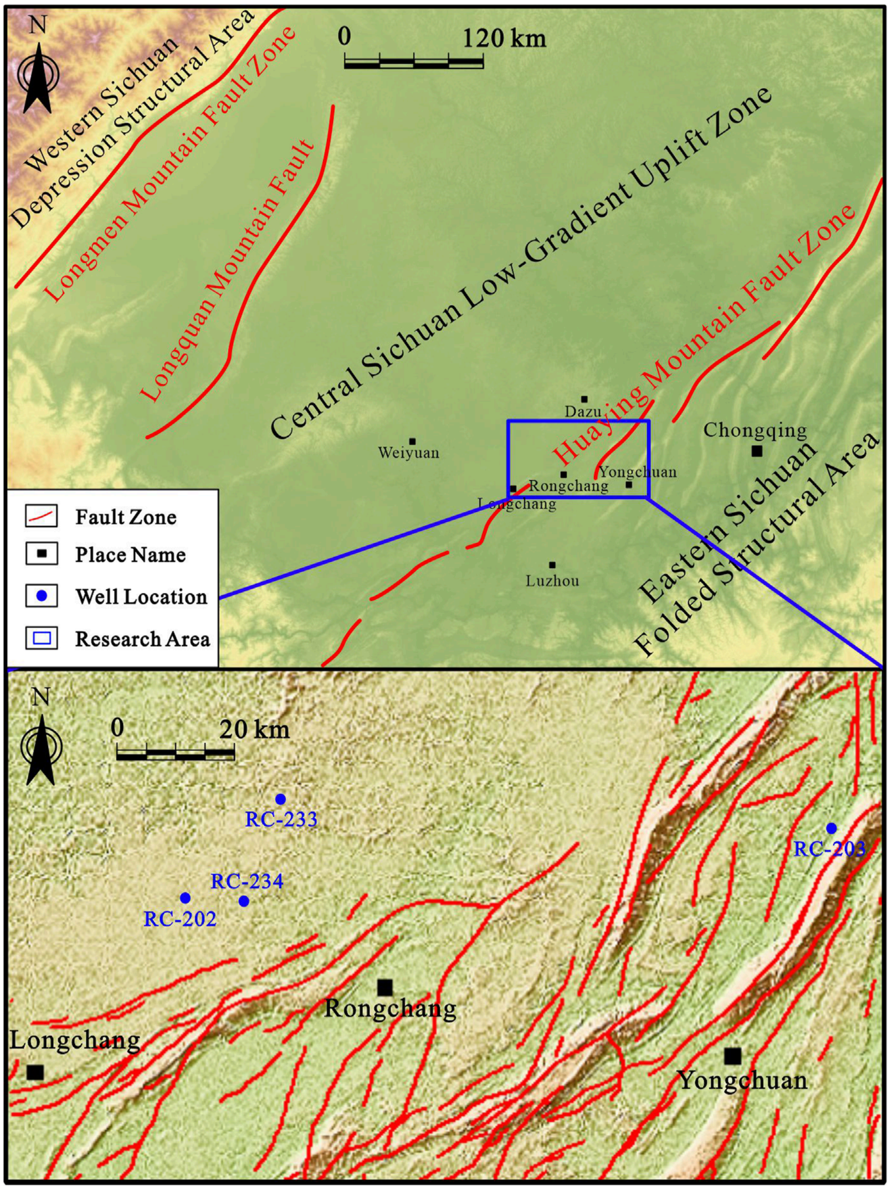

FIGURE 1
Location of the study area and distribution map of faults.

τ is the shear stress on the fault plane; μ is the friction coefficient; σn is the effective normal stress on the fault plane; Sn is the normal stress resolved on the friction surface; Pp is the pore pressure.

According to the CFF, the stability state of the fault plane can be determined: when the CFF is negative, the shear stress is insufficient to overcome the sliding resistance, and the fault plane remains stable; when the CFF reaches zero, the shear stress is equal to the sliding resistance, and the fault is in a critically stable state, with the possibility of sliding existing; when the CFF is positive, the shear stress is sufficient to overcome the sliding resistance, and the stability of the fault is destroyed, resulting in sliding (Chen, et al., 2021; Zoback, et al., 2003).

4 Evaluation of fault stability

4.1 Three-dimensional in-situ stress simulation analysis

The present-day *in-situ* stress values of the study area can be obtained through methods such as on-site measurement, experimental testing, logging calculation, numerical simulation, and obtaining the stress field by fitting the sliding direction of the seismogenic fault plane (Liu, et al., 2024; Li et al., 2024; Zheng, et al., 2017). This paper calculates the present-day *in-situ* stress field of the study area based on the finite element numerical simulation method (Qiao, et al., 2024; Zhou, et al., 2007). By comprehensively using the

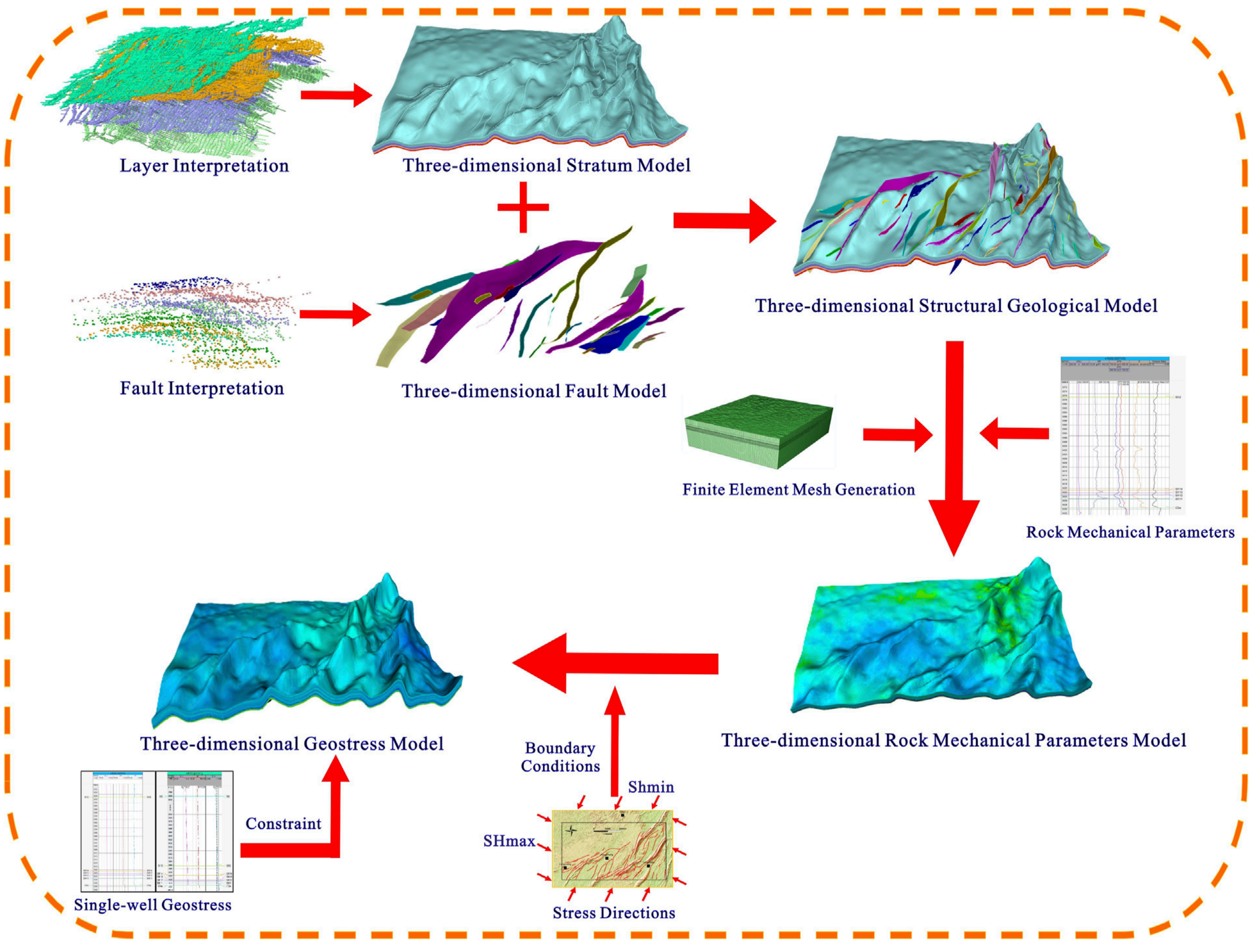

FIGURE 2
Flow chart of three-dimensional *in-situ* stress simulation.

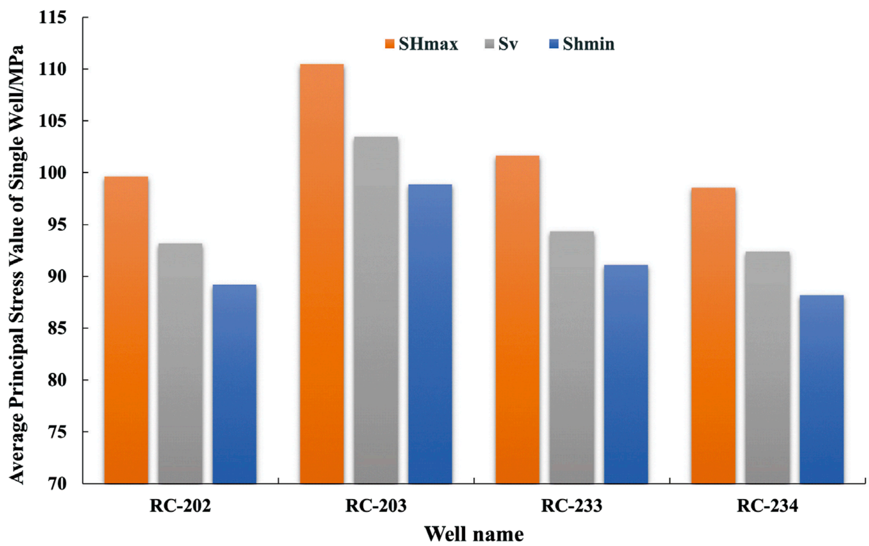

FIGURE 3
Distribution map of the principal stress of a single well.

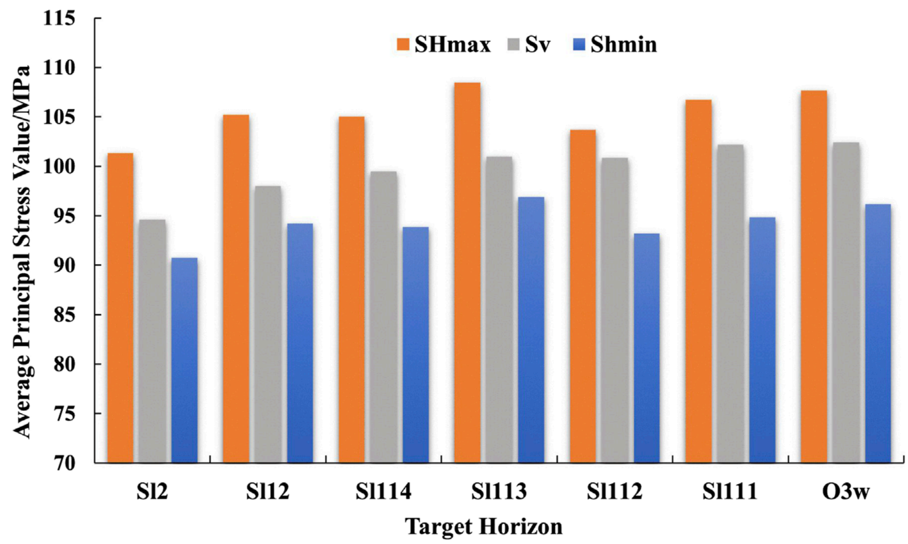

FIGURE 4
Distribution map of the principal stress of the target formation.

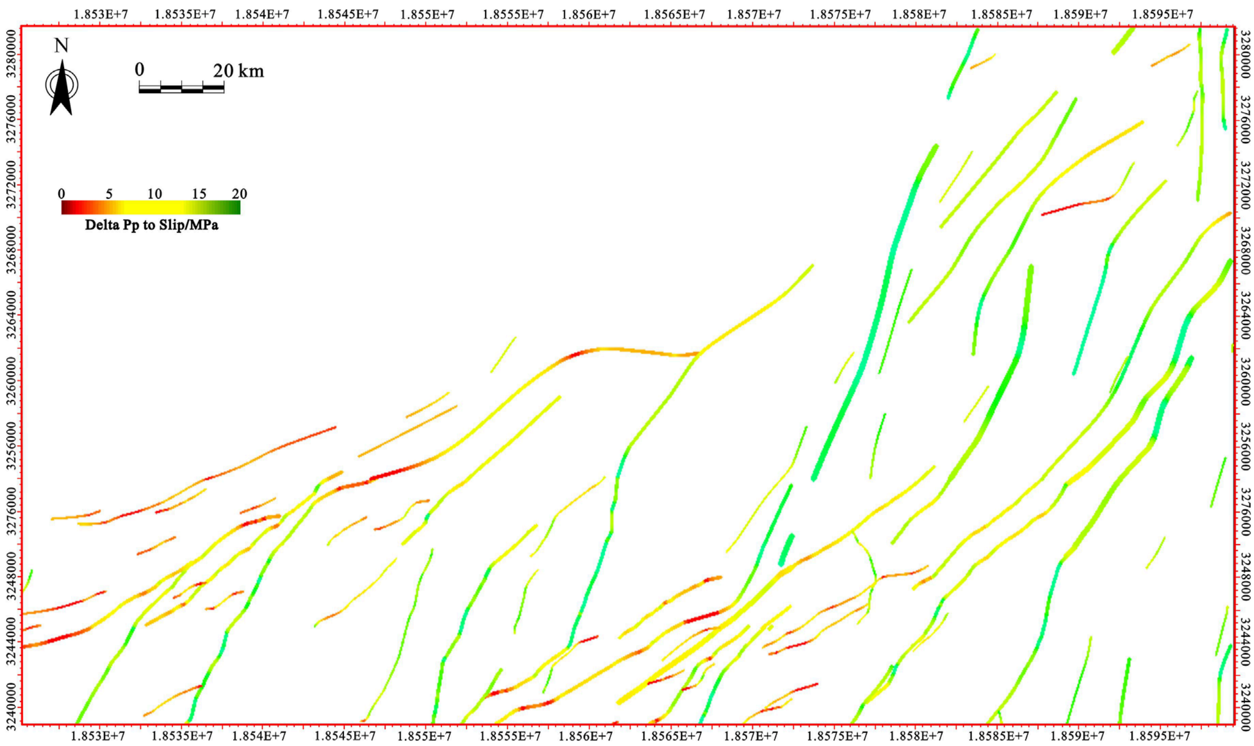

FIGURE 5
Results of the fault stability evaluation.

geological, logging, seismic and other data of the study area, a three-dimensional fine structural interpretation of the target formation in the study area is carried out. The intersecting relationships between faults, and between strata and faults are sorted out. A three-dimensional structural geological model of the study area is established. The structural model is subjected to three-dimensional finite element meshing. Combined with the rock mechanical parameters of single wells, a three-dimensional rock mechanical model is established. Furthermore, by using the *in-situ* stress test results of the target formation in the comprehensive study area and the *in-situ* stress analysis results of imaging logging, it is determined that the loading boundary condition for this stress simulation is

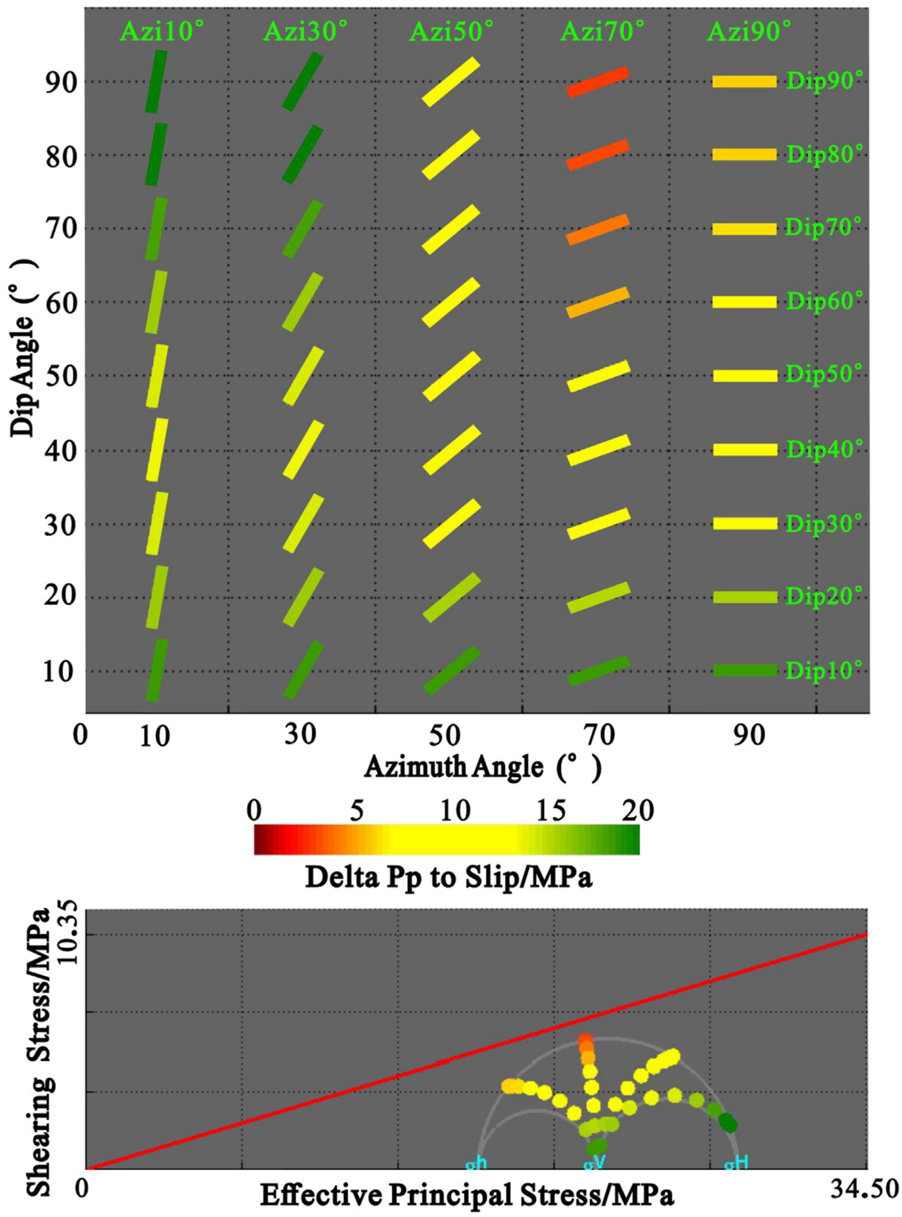

FIGURE 6
Simulation results of fault stability under different occurrences.

that the direction of the maximum horizontal principal stress is an azimuth angle of 110°. The numerical simulation of the present-day *in-situ* stress field of the study area is carried out to analyze the characteristics of the *in-situ* stress in the study area (Figure 2).

The results show that the main range of the principal stress SHmax of a single well in the study area is between 98 and 110 MPa, the main range of Shmin is between 88 and 98 MPa, and the main range of Sv is between 92 and 103 MPa (Figure 3). The main range of the *in-situ* stress SHmax of the target formation, the Wufeng Formation-Longmaxi Formation, is between 101 and 108 MPa, the main range of Shmin is between 93 and 97 MPa, and the main range of Sv is between 94 and 102 MPa. The magnitude of the principal stress in the study area shows the relationship of SHmax > Sv > Shmin (Figure 4).

According to the magnitude relationship among SHmax, Sv and Shmin, the stress environment of the study area is judged. When Sv > SHmax > Shmin, it indicates that the area is in a normal fault stress environment; when SHmax > Sv > Shmin, it indicates that the area is in a strike-slip fault stress environment; and when SHmax > Shmin > Sv, it indicates that the area is in a reverse fault stress environment (Anderson, 1951; Brooke-Barnett et al., 2015). Therefore, the relative magnitude relationship of the present-day stress in the study area is SHmax > Sv > Shmin, indicating that the area belongs to a typical strike-slip stress environment.

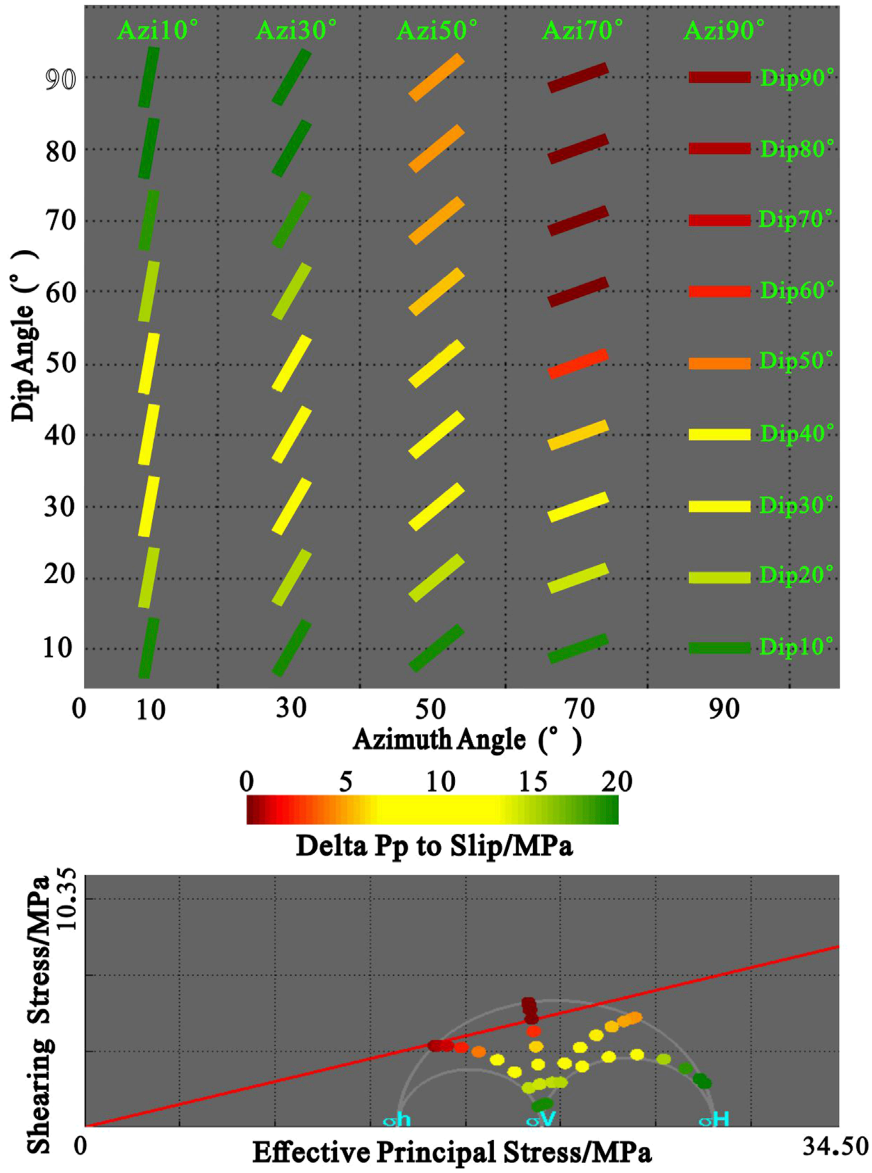

FIGURE 7
Stability simulation under 80 MPa pore pressure.

4.2 Evaluation of fault stability

Based on the present-day *in-situ* stress field of the study area and Coulomb's fault slip theory, and combined with the characteristics of the faults, an evaluation of fault stability is carried out. The results show that there are significant differences in the stability of different faults. Generally speaking, the faults in the western and southern parts of the study area have poor stability, while the faults in the northeastern part have better stability. Through further analysis in combination with the occurrence of the faults, the faults trending in the north-northeast direction generally have good fault stability; the faults trending in the northeast and north-northeast directions have relatively poor stability (Figure 5).

5 Discussion

Based on the results of the evaluation of fault stability, it is found that there are obvious differences in the stability along the same fault. At the same time, during fracturing development, the injection of high-pressure fluids will lead to changes in pore pressure, which in turn will cause changes in the effective normal stress and result in changes in fault stability (Li, et al., 2024; Hui, et al., 2021; Chen, et al., 2021). Therefore, it is necessary to explore the influence of fault occurrence and pore pressure on fault stability, and establish a model for the stability of fault occurrence and pore pressure in the study area.

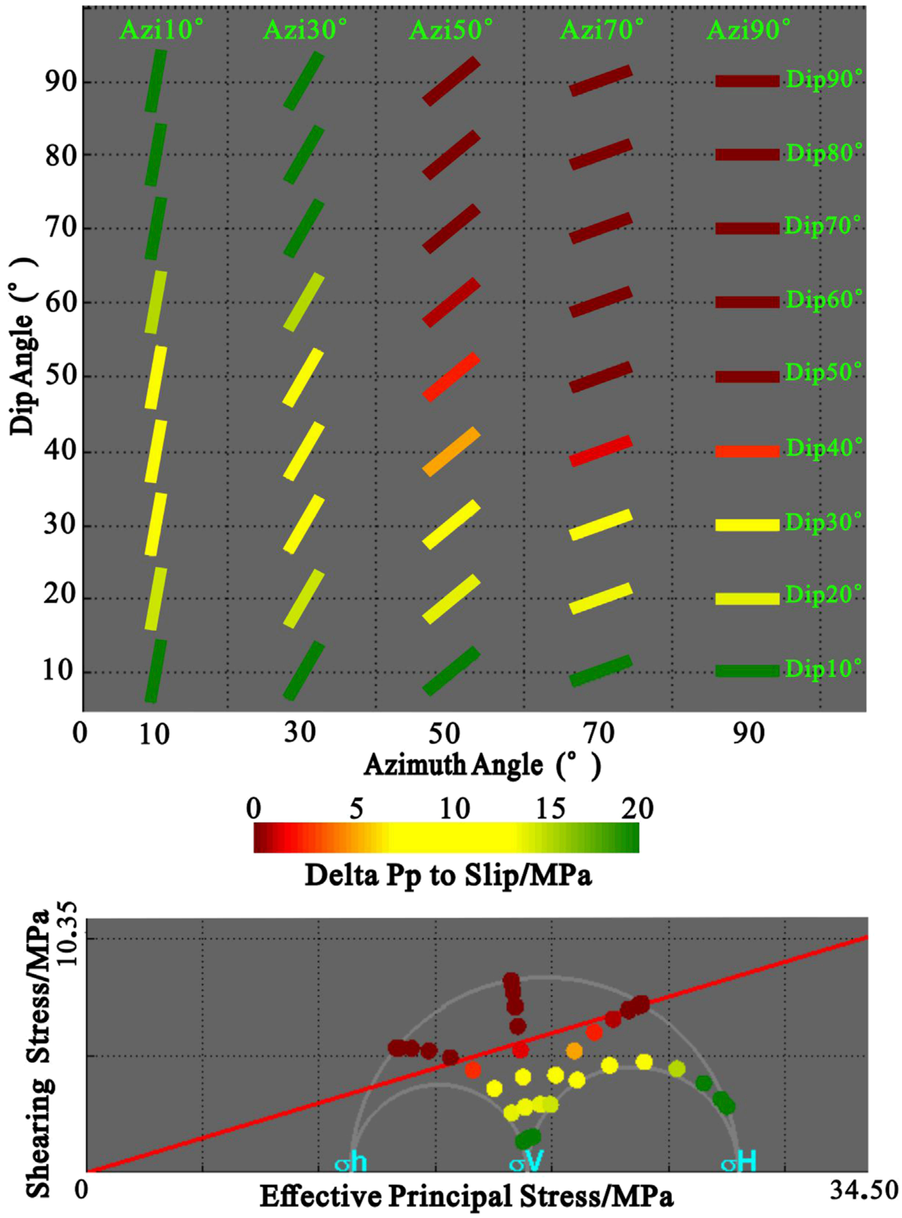

FIGURE 8
Stability simulation under 85 MPa pore pressure.

5.1 The influence of fault occurrence on fault stability

According to the fault occurrence situation in the study area, the range of the fault azimuth angle is set to be from 10° to 90°, with an interval of 20°, and the range of the dip angle is from 10° to 90°, with an interval of 10°. By analyzing the measured pressure data in the study area, the formation pore pressure is determined to be 75 MPa. A fault model is established to explore the influence of fault occurrence on fault stability. The simulation results show that there are obvious differences in the fault stability of faults with different occurrences. Specifically (Figure 6), when the fault dip angle is less than 10°, and for faults with an azimuth angle less than 30° and a dip angle greater than 60°, the fault stability is the best; when the fault azimuth angle is greater than 50°, with the increase of the dip angle, the fault stability gradually decreases, and when the fault azimuth angle is 70° and the dip angle is greater than 70°, the stability of the faults with this occurrence is the worst. The results indicate that the fault occurrence is a key factor affecting fault stability.

5.2 The influence of pore pressure on fault stability

Pore pressure has an important influence on fault stability. In order to deeply explore how pore pressure affects the fault stability

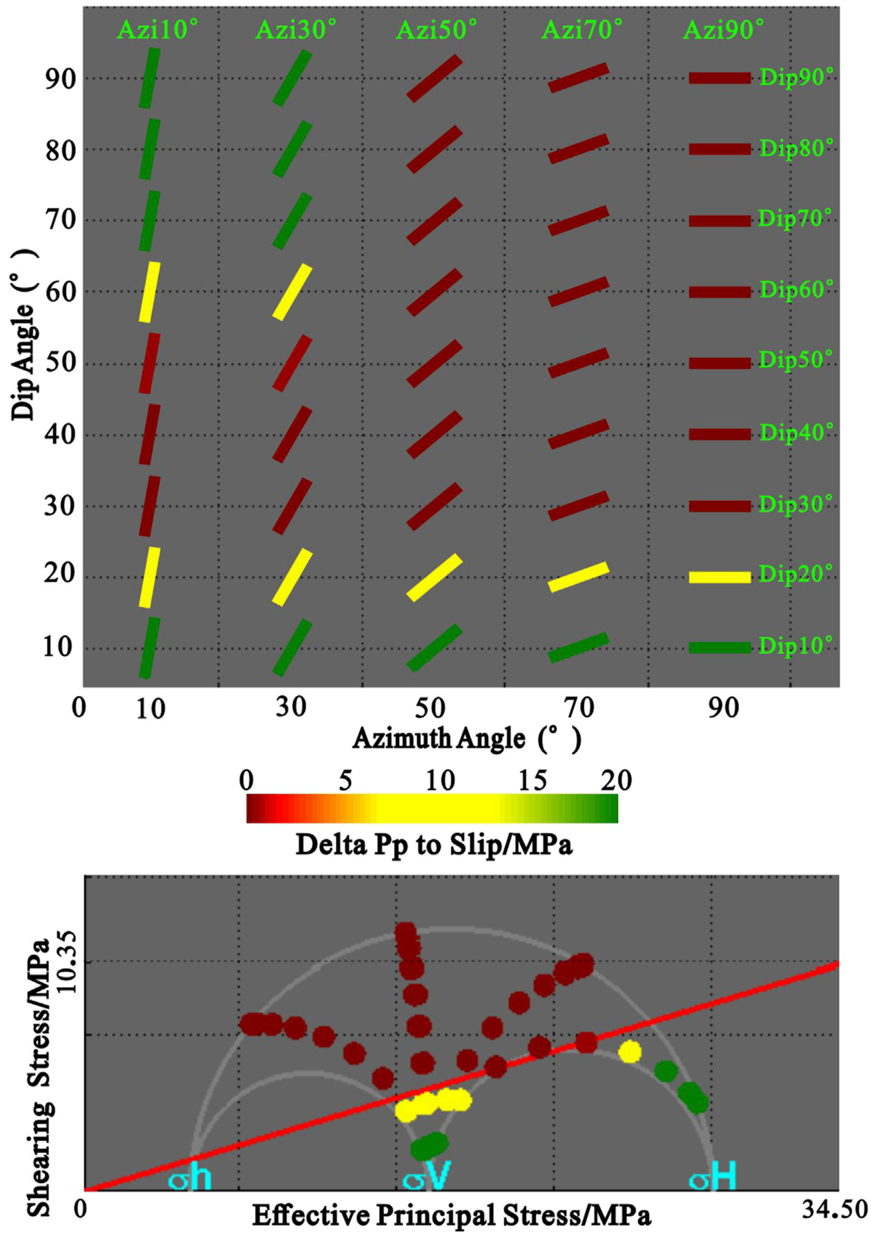

FIGURE 9
Stability simulation under 90 MPa pore pressure.

in the study area, based on the fault model of the study area, the simulation of fault stability is carried out by gradually increasing the formation pore pressure in the study area. First, the pore pressure is increased from 75 MPa to 80 MPa for the simulation of fault stability. The results show that for the faults in the study area with an azimuth angle greater than 70° and a dip angle greater than 60°, they cross the fault instability line on the Mohr circle, and the faults slip; when the azimuth angle is 50°, with the increase of the dip angle, the fault stability gradually deteriorates; while for the fault occurrences with a dip angle less than 10° and an azimuth angle less than 30° and a dip angle greater than 60°, the fault stability is the best (Figure 7).

Furthermore, the pore pressure in the study area is increased to 85 MPa for the simulation of fault stability (Figure 8). Compared with the simulation results at a pore pressure of 80 MPa, the number of unstable faults in the study area increases significantly, and the number of faults with deteriorated stability also increases, which has a significant impact on the fault stability. Specifically, for the faults within the range of an azimuth angle greater than 50° and a dip angle greater than 50°, they cross the fault instability line on the Mohr circle, and the faults slip; for the faults with a dip angle in the range of 30°–50°, their fault stability decreases with the increase of the azimuth angle; when the fault occurrence is with an azimuth angle greater than 50° and a dip angle of about 40°, the faults with this occurrence are in a critical state of sliding; when the fault dip angle is less than 10° and the azimuth angle is less than 30° and the dip angle is greater than 70°, the fault stability is the best.

When the pore pressure in the study area is increased to 90 MPa (Figure 9), the results show that for the faults with an occurrence of an azimuth angle greater than 50° and a dip angle greater than 30°, as well as those with an azimuth angle less than 30° and a dip angle between 30° and 50°, these faults have crossed the fault instability line on the Mohr circle, and the faults become unstable and slip; when the dip angle is less than 10°, the azimuth angle is less than 30°, and the dip angle is greater than 70°, the fault stability is the best.

In conclusion, as the pore pressure increases, the fault stability gradually decreases, and the ranges of the azimuth angle and dip angle of the unstable faults gradually expand. Specifically, when the pore pressure is increased by 5 MPa, the faults in the study area with an occurrence within the range of an azimuth angle greater than 70° and a dip angle greater than 60° slip first; when the pore pressure is increased by 10 MPa, the faults within the range of an azimuth angle greater than 50° and a dip angle greater than 50° become unstable and slip; when the pore pressure is increased by 15 MPa, the faults with an occurrence of an azimuth angle greater than 50° and a dip angle greater than 30°, and those with an azimuth angle less than 30° and a dip angle between 30° and 50° become unstable and slip. The research results provide a basis for avoiding potential risks and achieving efficient development during the development of shale gas.

6 Conclusion

(1) The main range of the principal stress SHmax of a single well in the Rongchang area is between 98 and 110 MPa, the main range of Shmin is between 88 and 98 MPa, and the main range of Sv is between 92 and 103 MPa. The main range of the *in-situ* stress SHmax of the target formation, the Wufeng Formation-Longmaxi Formation, is between 101 and 108 MPa, the main range of Shmin is between 93 and 97 MPa, and the main range of Sv is between 94 and 102 MPa. The magnitude of the principal stress in the study area shows the relationship of SHmax > Sv > Shmin. The relative magnitude relationship of the present-day stress is SHmax > Sv > Shmin, which belongs to a typical strike-slip stress environment.

(2) The distribution characteristics of the Huayingshan Fault in the Rongchang area are that it converges in the northeast direction and diverges in the southwest direction, presenting a broom shape. The fault stability of the faults in the western and southern parts of the study area is poor, while the stability of the faults in the northeastern part is better, and there are differences in stability along the same fault.

(3) In the Rongchang area, the faults with a dip angle of less than 10°, and the faults with an azimuth angle of less than 30° and a dip angle of greater than 60° have good stability. For the faults with an azimuth angle greater than 50°, their stability decreases as the dip angle increases. When the azimuth angle is 70° and the dip angle is greater than 70°, the stability is poor. Currently, all the faults in the study area remain stable, and it is clear that the fault occurrence is a key factor affecting fault stability.

(4) As the pore pressure increases, the ranges of the azimuth angle and dip angle of the unstable faults gradually expand. The azimuth angle decreases from greater than 70°–50°, and the dip angle decreases from 60° to 30°. At the same time, the faults with an azimuth angle of less than 30° and a dip angle between 30° and 50° also become unstable and slip, indicating that the pore pressure is an important factor affecting fault stability.

Data availability statement

The original contributions presented in the study are included in the article/supplementary material, further inquiries can be directed to the corresponding authors.

Author contributions

SH: Writing–original draft. YT: Investigation, Writing–review and editing. ZQ: Validation, Writing–review and editing. XF: Writing–review and editing. YM: Writing–original draft.

Funding

The author(s) declare that no financial support was received for the research, authorship, and/or publication of this article.

Conflict of interest

Author ZQ was employed by Geophysical Prospecting Research Institute of Jiangsu Oilfield Company, Sinopec.

The remaining authors declare that the research was conducted in the absence of any commercial or financial relationships that could be construed as a potential conflict of interest.

Generative AI statement

The author(s) declare that no Generative AI was used in the creation of this manuscript.

Publisher's note

References

Anderson, E. M. (1951). *The dynamics of faulting and dyke formation with applications to Britain*. second edition. Oliver: Elsevier, 206.

Brooke-Barnett, S., Flottmann, T., Paul, P. K., Busetti, S., Hennings, P., Reid, R., et al. (2015). Influence of basement structures on *in-situ* stresses over the Surat Basin, southeast Queensland. *J. Geophys. Res.* 120 (7), 4946–4965. doi:10.1002/2015jb011964

Chen, C., Zhang, H., and Zhou, X. (2021). Analysis of microseismic characteristics of shale gas casing deformation wells in Changning, Sichuan. *Pet. Geophys. Explor.* 56 (06), 1286–1292 + 1198. doi:10.13810/j.cnki.issn.1000-7210.2021.06.010

He, V., and Spiers, C. J. (2011). The frictional sliding properties and implications of sedimentary rocks and natural fault gouge in Longmenshan fault zone. *J. Rock Mech. Eng.* 30 (01), 113–131.

Hui, G., Chen, S., and Gu, F. (2021). Fluid-geomechanical coupling modeling to characterize hydraulic fracturing-induced earthquakes: a case study of Fox Creek, Canada. *Accord. Geophys. J.* 64 (03), 864–875.

Jiang, H. (2021). *The control of tectonic evolution on the differential enrichment of shale gas in the Longmaxi Formation in southern Sichuan*. Beijing: China University of Petroleum.

Jiang, L., Pu, J., and Ding, Y. (2024). Research on fault activity in the northern Rongchang area. *Energy Environ.* (05), 51–53.

Jiang, Z., Liang, Z., and Shen, Y. (2023). Coupling relationship and research direction of key elements of geological engineering integration of shale gas dessert in Luzhou area, southern Sichuan. *Geoscience* 48 (01), 110–129.

Ju, W., Wang, J., Fang, H., Gong, Y., and Zhang, S. (2017). Paleostress reconstructions and stress regimes in the Nanchuan region of Sichuan Basin, South China: implications for hydrocarbon exploration. *Geosciences J.* 21 (4), 553–564. doi:10.1007/s12303-016-0066-1

Lei, X., Li, X., and Li, Q. (2014). The role of small faults in sedimentary rock storage systems in water-flooding-induced seismicity in oil and gas fields-a case study of the Sichuan Basin. *Seismogeology* 36 (03), 625–643.

Li, X., Li, S., and He, J. (2024). An introduction to geomechanics of reservoir engineering. *J. Eng. Geol.* 32 (04), 1155–1175.

Li, X., Zhang, G., and Xie, Z. (2022). The seismogenic mechanism and temporal and spatial evolution characteristics of seismic activity of the M6.0 earthquake in Luxian County, Sichuan Province in 2021. *Accord. Geophys. J.* 65 (11), 4284–4298.

Li, Z., Wan, Y., and Guo, X. (2024). The significance of accurately identifying the seismogenic fault plane from the focal mechanism for reconstructing the stress field. *Geophys. J.* 67 (07), 2612–2624.

Liu, G., Lu, H., and He, S. (2009). Review of *in-situ* stress research on oil and gas reservoirs by finite element method. *Sci. Technol. Eng.* 9 (24), 7430–7435.

Liu, Y., Ju, W., and Xiong, W. (2024). Current *in-situ* stress characteristics and shale gas development of Wufeng-Longmaxi Formation in Luzhou block, southern Sichuan. *Sci. Technol. Eng.* 24 (08), 3200–3206.

Qiao, H., Zhang, Y., and Nie, H. (2024). Multi-scale natural fracture characterization and three-dimensional geological modeling of shale reservoirs: a case study of the Wufeng-Longmaxi Formation shales in the Pingqiao structural belt, Sichuan Basin. *Geol. Front.* 31 (05), 89–102. doi:10.13745/j.esf.sf.2023.6.13

Yi, G., Long, F., and Liang, M. (2019). Focal mechanism solution and seismogenic structure analysis of the MS6.0 earthquake sequence in Changning, Sichuan Province on June 17,2019. *Chin. J. Geophys.* 62 (09), 3432–3447.

Yi, Gi, Long, F., and Liang, M. (2020). Geometric structure and tectonic deformation characteristics of seismogenic structure in Rongxian-Weiyuan-Zizhong area of Sichuan Basin: understanding and enlightenment based on focal mechanism solution. *Accord. Geophys. J.* 63 (09), 3275–3291.

Zhang, H., Yin, G., and Wang, H. (2019). Influence of geomechanical response of natural fractures on gas well productivity in Kuqa Depression, Tarim Basin. *Nat. Gas. Geosci.* 30 (03), 379–388.

Zhang, J., Kuang, W., and Zhang, X. (2021). Research status and countermeasures of earthquake induced by global oil and gas exploitation. *Earth Planet. Phys. Rev.* 52 (03), 239–265. doi:10.19975/j.dqyxx.2020-027

Zhang, Z., Zeng, X., and Wang, D. (2024). Study on the pre-earthquake stress state before the MS6.1 Lushan earthquake in Sichuan in 2022. *Seismol. Res.* 47 (04), 483–492. doi:10.20015/j.cnki.ISSN1000-0666.2024.0061

Zheng, D., Xu, H., and Wang, J. (2017). Key technologies for the construction and evaluation of gas storage. *Petroleum Explor. Dev.* 44 (05), 794–801.

Zhou, W., Yan, C., and Wang, S. (2007). *Evaluation method and application of present stress field in oil and gas reservoir*. Beijing: Geological Publishing House, 179.

Zhu, H., Lu, Y., Pan, Y., Qiao, P., Raza, A., and Liu, W. (2024). Nanoscale mineralogy and organic structure characterization of shales: insights via AFM-IR spectroscopy. *Adv. Geo-Energy Res.* 13 (3), 231–236. doi:10.46690/ager.2024.09.08

Zoback, M., Barton, C., Brudy, M., Castillo, D., Finkbeiner, T., Grollimund, B., et al. (2003). Determination of stress orientation and magnitude in deep wells. *Int. J. Rock Mech. Min. Sci.* 40 (7), 1049–1076. doi:10.1016/j.ijrmms.2003.07.001